DEVELOPMENT OF A WIDE-VIEW VISUAL PRESENTATION SYSTEM AND ESTIMATING HUMAN PRIMARY VISUAL CORTICAL MAGNIFICATION BY USING FMRI FOR TRAFFIC SAFETY

Jinglong WU
Professor and Lab. Head, Bio-Measurement Engineering Laboratory Division of Industrial Innovation Sciences, The Graduate School of Natural Science and Technology, Okayama University, Okayama, Japan

Fengzhe JIN
Graduate School of Engineering, Kagawa University Kagawa, Japan

Takanori KOCHIYAMA
Brain Activity Imaging Center, ATR Kyoto, Japan

Masafumi YANO
Director, Research Institute of Electrical Communication Tohoku University Miyagi, Japan

Kazumi RENGE
Professor, Department of Psychology Faculty of Psychology and Welfare Tezukayama University Nara, Japan

It is very important to understand human visual characteristics in the wide-view condition for traffic safety. In the present study, we focus on human basic visual characteristics of retinotopic mapping by using functional Magnetic Resonance Imaging (fMRI), and provide basic research results for traffic safety.

Previous fMRI studies on human visual retinotopic mapping are typically used for central and/or peri-central visual field stimulus. The retinotopic characteristics on human peripheral vision are still not well known. In this study, we developed a new visual presentation system widest view (60 degrees of eccentricity). The wide-view visual presentation system was made from nonmagnetic optical fibers and a contact lens, so it can used in general clinical fMRI conditions and the cost is lower.

In the present study, by using the newly developed wide view visual presentation system, we have firstly been able to gain success in the world to identify the human primary visual cortex (V1) with an eccentricity of 60 degrees and the quantitative relationship between V1 and peripheral visual field (eccentricity up to 60 degrees) by fMRI. In addition, we estimated the mean area for the V1 between 0-60 degree eccentricities, and acquired the areal cortical magnification function for V1 between 0-60 degree eccentricities was $M_{areal} = 272/(E+1.44)^2$. The mean cortical surface area of V1 between the 0-60 degree eccentricities was about 2229 mm^2. Our results have good agreement with using physiological, patient and anatomical measurements.

From the results of the present study, it is explained why traffic accidences easily take place on crossings. In the human brain visual cortex (V1), only a small cortical area is used to process visual information from the peripheral visual field. The basic results suggest that drivers are unable to recognise the dangerous information from both sides of peripheral vision.

Key Words: Traffic safety, Peripheral visual field, Primary visual cortex, functional Magnetic Resonance Imaging (fMRI)

1. INTRODUCTION

In Japan, more than 5000 people die due to traffic accidents every year. In 2007, there were a total of 832,454 traffic accidents, and the number of injured persons was 1,034,445 and 5,744 persons died[1]. Statistical analysis showed that crossroads and old people are two factors which cause traffic accidents[1]. At a crossroad, drivers need to observe the surrounding situation of both sides by using their peripheral vision. Previous research has shown that the vision of the elderly will decline with an increase in age[2,3]. So it is important from the view of traffic safety to study the characteristics of peripheral vision of the human brain.

In the human visual pathway, visual information passes from the retina to the lateral geniculate nucleus and then to the human primary visual cortex. Therefore, the human primary visual cortex (V1) contains a map of visual space. To a good approximation, each two-dimensional (2D) location in the visual field is represented at a single physical location within V1. Some researchers tried to realize retinotopic mapping using functional magnetic resonance imaging (fMRI). Previous human retinotopic studies by fMRI have identified the V1[4-6], placing it between the occipital pole and the lateral end of the parieto-occipital sulcus (POS). Some results were observed by the use of visual stimuli mainly limited to central and/or peri-central visual fields from 8° to 30° of eccentricity by

fMRI studies. Such stimuli do not directly activate much of the periphery in V1. Consequently, the anatomical and physiological characteristics of human peripheral vision above 30° of eccentricity are still not clear from the fMRI study.

The cortical magnification factor was defined by Daniel and Whitteridge to be the distance in the cortex (in millimeters) devoted to representing a step of 1 degree in visual space[7]. Therefore, the cortical magnification factor is correlated with the characteristics of visual field. If the mapping function is analyzed in detail, then the magnification factor represents the magnitude of the derivative of the mapping. The area of cortical magnification (the area of cortical surface in mm^2 per area of visual field in deg^2) is often described by the function: $M_{areal} = a/(E+b)^2$ for V1, where E indicates eccentricity in degrees, and a and b are constants.

Many studies have typically used a cortical magnification factor to quantify the relationship between the V1 surface area and a visual field and have indicated that the cortical magnification factor within the human V1 is correlated with visual acuity thresholds[8]. Therefore, by estimating a cortical magnification factor, we can compare central and peripheral visual performances in humans.

In this study, we developed a wide-view visual stimulus presentation system and used it for mapping the human retinotopic organization of the far peripheral visual field up to 120° larger than the previous 60° by fMRI. We also estimated the cortical surface area of the V1. We used fMRI to examine the areal cortical magnification from 0° to 60° of eccentricity to investigate the quantitative relationship between the V1 surface area and human peripheral visual field. Our results are used to discuss the relationship of peripheral vision and traffic safety.

2. DEVELOPMENT OF A WIDE-VIEW VISUAL PRESENTATION SYSTEM

The visual stimuli presentation system shown in Figure 1 consists of the entrance apparatus and the presentation apparatus. The entrance apparatus includes a section of optical fiber bundles (CK-20, Eska; Mitsubishi, Japan) supported by a stand, a DLP projector (UPS-100; PLUS, Japan) by which stimuli are projected onto the fiber bundle section, and a personal computer (CF-R4; Panasonic, Japan) used to control the stimulus presentation sequence. Figure 2 shows the entrance apparatus. As shown in Figure 3, the presentation apparatus contains the stimulation transmission optical fiber bundles and the
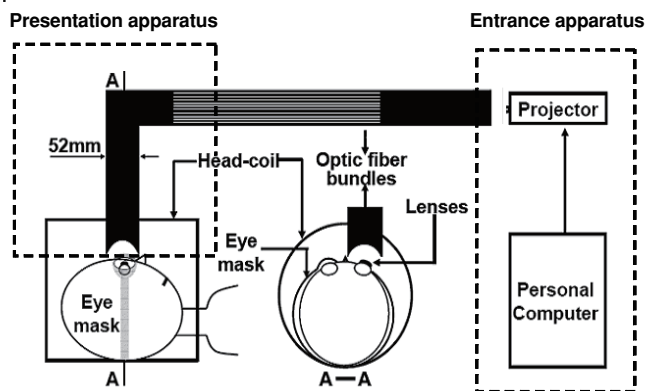

Fig. 1 Visual stimuli presentation system includes an entrance apparatus and a presentation apparatus which are surrounded by the dashed line respectively. The center graph is broken-out section of A which is marked in the system.
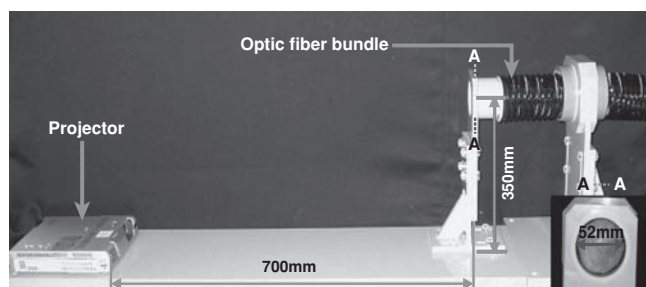

Fig. 2 The entrance apparatus includes an optical fiber bundle, a projector and a personal computer. The projector is 700 mm away from the fiber bundles. The computer is used to produce the presentation stimuli. The stimuli are projected onto the fiber bundles by the projector. The right-bottom graph is the broken-out section of A which is marked in the apparatus.

structure used to fix the fiber bundles. The optical fiber bundle, composed of a 0.5-mm-diameter optical fiber, has a diameter of 52 mm and a length of approximately 5,500 mm. A flexible plastic sleeve is used to protect the fiber bundle. Black tape, fixed to the outside of the plastic sleeve, prevents light leakage between the fiber bundle and outside environment. The optical fiber bundles of the entrance apparatus are comprised of a flat surface, but the screen has a curved surface with a radius of 30 mm. The whole system is made of nonmagnetic polyester plastic, preventing any influence from the magnetic field of the MRI. Inside the scanner, a plastic optical bundle holder rests on the head coil and supports the optical bundle. The holder is made of non-ferrous materials (PVC).
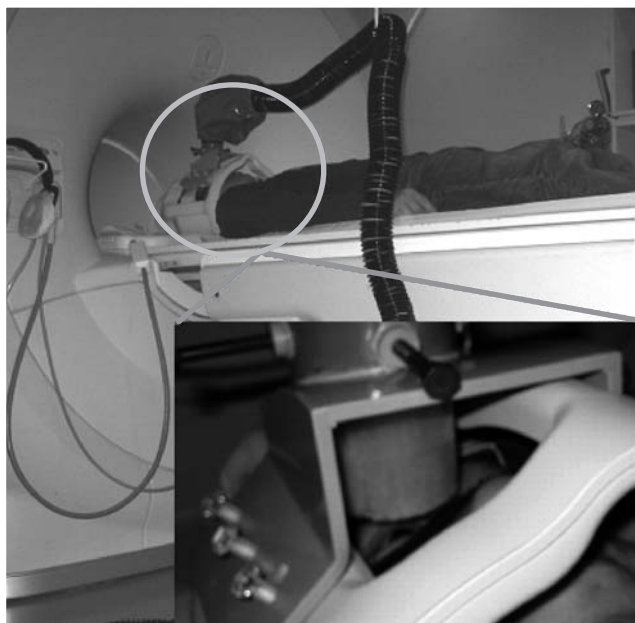
Fig. 3 Presentation apparatus contains the stimulation transmission optical fiber bundles and the structure used to fix the fiber bundles. The right-bottom graph is an enlarged drawing of red circled area, which is marked in the apparatus.

It is easy to set up and remove, and allows adjustment of the optic bundle position to accommodate various head sizes, eye positions, and interpupillary distances. The distance from the center of the optical fiber bundle screen to the eye is 30 mm.

3. MATERIALS AND METHODS

3.1 Subjects and stimuli

Eight healthy subjects without previous neurological or psychiatric disorders (age 19–31 years, mean 25 years; two women, six men) participated in the study. The subjects had normal or corrected-to-normal vision and were right-handed. We obtained written informed consent from all subjects before the experiment. The study was approved by the Institutional Research Review Board of Kagawa University, Japan.

Visual stimuli were created on a display using a resolution of 800 × 600 pixels. The display stimulus was brought to the subject's eyes within the scanner by a wide-view optical-fiber presentation system. Monocular (right eye) presentations were accomplished; the optical-fiber screen (surface-curved with a radius of 30 mm) was placed in the center of the 30 mm radius from a subject's eye. The visual field of stimulus was 120° horizontal ×
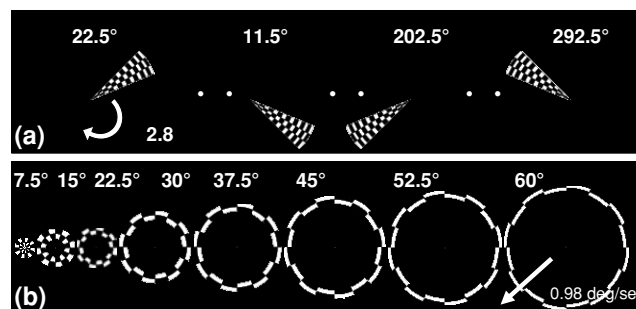

Fig. 4 Rotating and expanding visual stimuli. (a: is the rotating stimulus which is a wedge with checkerboard pattern rotating in steps of 22.5°, b: is the expanding stimulus which is a ring with a checkerboard pattern moving from the center to the periphery in 7.5° steps)

120° vertical. Because the screen was so close to the eye, subjects wore a contact lens (Menicon soft MA; Menicon, Japan. with 20×, 22×, 25× magnification) to retain their length of focus.

To identify the retinotopic areas of the visual cortex, we carried out fMRI scans while subjects viewed phase-encoding stimuli[4-6,9]. A high-contrast, black-and-white, radial checkerboard pattern (mean luminance 110cd/m^2, contrast 97%) reversed contrast at a frequency of 8 Hz, with eccentricity ranging from 0° to 60° visual angles. As shown in Figure 4, two types of stimulus were used for locating visual area boundaries and estimating eccentricity. In Figure 4a, the stimulus for locating boundaries was a 22.5° wedge that rotated slowly counterclockwise about a red fixation spot at the center of the stimuli. The wedge rotated in steps of 22.5°, remaining in each position for 4s before instantaneously rotating to the next position. In Figure 4b, the stimulus for estimating eccentricity was an expanding checkered annulus. The flickering radial checkerboard was moved from the center to the periphery in discrete steps (each step 7.5°, with a total of eight steps), remaining at each position for 8s before instantaneously expanding to the next position. Each experimental run lasted 300s. In each run, four complete rotations and expansions of the flickering checkerboard were presented. Six such runs were conducted, three using wedges and another three using rings. All experiments used passive viewing, and subjects were required to maintain fixation throughout the period of scan acquisition. To minimize head motion, each subject's head was stabilized with foam pads. All subjects wore a black mask to cover the left eye.

3.2 MRI data acquisition

The fMRI experiment was performed using a 1.5 T Philips clinical scanner (Intera Achieva; Best, The Netherlands). All images were acquired using a standard radio-frequency head coil. We acquired 23 slices approximately orthogonal to the calcarine sulcus of the brain to cover most of the cortical visual areas. The T2*-weighted gradient echo-planner imaging sequence was used with the following parameters: TR/TE = 2000/50 ms; FA = 90°; matrix size = 64 × 64; and voxel size = 3 × 3 × 3 mm. Before acquiring the functional images, T2-weighted anatomical images were obtained in the same planes as the functional images, using the spin echo sequence. A T1-weighted high-resolution image was also acquired after each functional experiment.

3.3 Data analysis

The functional and anatomical data were processed using the BrainVoyager software package (Brain Innovation, Masstricht, Netherlands). After preprocessing the functional data, anatomical data was processed. The recorded high-resolution T1-weighted three-dimensional (3-D) recordings were used for surface reconstruction. The gray and white matter was segmented using a region-growing method, and the gray matter cortical surface was reconstructed. Prior to surface flattening, the cortical surface was inflated and cut along the calcarine sulcus from the occipital pole to slightly anterior of the POS[10].

The functional data were aligned onto the 3-D anatomic image using the image coordinates. To identify boundaries (wedge stimuli), maps were created based on cross-correlation values for each voxel, determined by a standard hemodynamic box-car function (r ≥ 0.2). We identified the boundaries of the V1 by hand based on the horizontal and vertical meridians and knowledge of the retinotopic organization of the visual cortex[11].

All volume measurements were made on the 3-D anatomical image. Under each eccentricity condition (0°–7.5°, 7.5°–15°, 15°–22.5°, 22.5°–30°, 30°–37.5°, 37.5°–45°, 45°–52.5°, 52.5°–60°), each strongest-response voxel in the V1 was counted as active for each 3-D anatomical image. Because the voxel size is 1 × 1 × 1 mm, the active voxel volume in the V1 for each eccentricity condition equals the counted number of voxels. If we assume that cortical thickness was invariable in the V1, then the V1 surface area can be obtained by dividing the voxel volume by the cortical thickness, assumed here to be 2.5 mm[12].

4. RESULTS

4.1 Eccentricity representation

We conducted eccentricity mapping for the human visual cortex. Figure 5 shows a color plot of one subject's response to the expanding ring stimulus in both hemispheres. The color hue at each cortical surface point again indicates the response phase and is proportional to the eccentricity of the local visual field representation. As the expending ring stimulus moved from the fovea to the periphery of the retina, the locus of the responding neurons varied from posterior to anterior portions of the calcarine sulcus in what is referred to as the eccentricity dimension of retinotopy. The most peripheral representation was at the medial end of the POS. Similar results were obtained for all subjects.
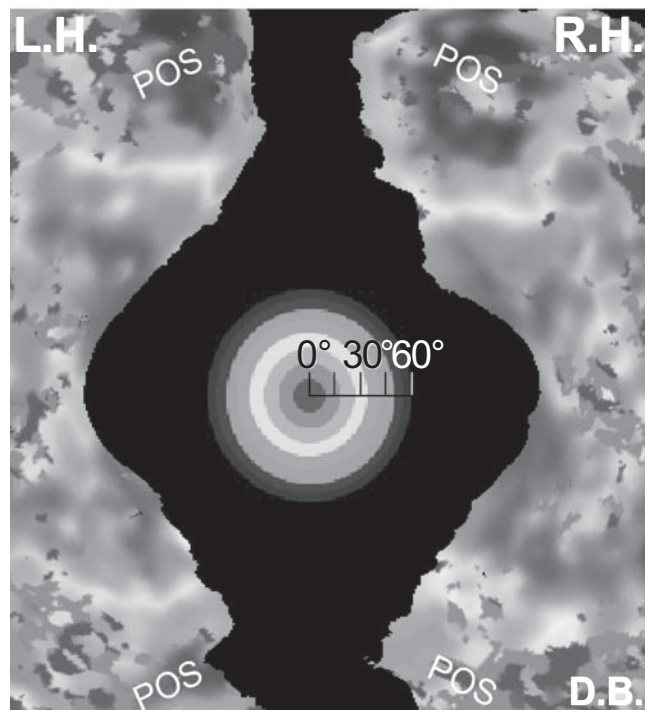

Fig. 5 Retinotopy of eccentricity representation in the visual cortex is shown by fMRI mapping. Phase-encoded eccentricity maps rendered on close-up views of the flattened left hemisphere (L.H.) and right hemisphere (R.H.) of one subject (D. B). The hue of the color at each cortical surface point indicates the response phase, which is proportional to the eccentricity of the local visual field representation (Center disk). Representations of central region through more peripheral eccentricities are coded using red, yellow, and blue, respectively. The peripheral representation arrives at the parieto-occipital sulcus (POS).

Table 1 Cortical surface area of V1

Subject	Hemisphere	Cortical surface area (mm^2)		
		Ventral	Dorsal	Total
1	Left	1175	1093	2268
	Right	1198	1178	2376
2	Left	1060	1194	2254
	Right	1121	1233	2354
3	Left	1268	1398	2667
	Right	1290	1098	2388
4	Left	955	1257	2211
	Right	1167	1333	2500
5	Left	916	925	1841
	Right	1249	1187	2435
6	Left	1171	1182	2353
	Right	1276	1069	2345
7	Left	704	1059	1763
	Right	853	938	1791
8	Left	836	954	1790
	Right	1137	1197	2334
	mean±s.e.m	1086±64	1143±48	2229±99

4.2 Surface area

Table 1 lists measurements of the V1 surface area representing the Eccentricity from 0° to 60°. The V1 surface area was estimated by the number of active voxels under all eight eccentricity conditions divided by the average cortical thickness (2.5 mm). Values for right and left hemispheres, dorsal and ventral aspects are listed separately for each subject. A one-block (8 subjects) two-way (2 hemispheres, 2 anatomical positions) ANOVA revealed no significant difference between the left and right hemisphere V1 surface areas [F(1, 21) = 4.248; P = 0.052] and no significant difference between the dorsal and ventral region V1 surface areas [F(1, 21) = 1.894; P = 0.183].

Surface area estimates of V1 based on V1 representation of the visual field for 0° to 60° eccentricity. The measurements are shown for the right and left hemispheres and dorsal and ventral aspects of V1 in the eight subjects (16 hemispheres). Various summary statistics are listed at the bottom of the table. The V1 surface area was based on the number of active voxels for the eight eccentricity conditions divided by the average cortical thickness (2.5 mm).

4.3 Areal cortical magnification

Figure 6 shows areal cortical magnification[13] functions from the current data, across all hemispheres imaged compared to data from Horton and Hoyt[14]. In this figure, the solid line denotes the data from this study, and the error bar indicates the standard error for all hemispheres. The dotted line shows results from Horton and
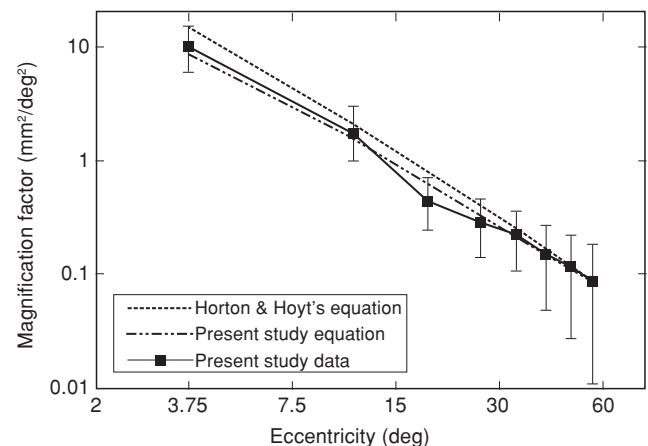

Fig. 6 Area cortical magnification functions from data acquired from all hemispheres imaged. The solid line indicates data from this study. The error bar denotes the standard error for all hemispheres. The dotted line shows results by Horton and Hoyt's[14] patients study, $M_{areal} = 300/(E + 0.75)^2$, and the line with the long dash and double dots represents the data from this study applied to the best-fit equation, $M_{areal} = 272/(E + 1.44)^2$.

Hoyt's[14] equation $M_{areal} = 300/(E + 0.75)^2$, and the dashed, double-dotted line shows our data for the best-fit equation $M_{areal} = 272/(E + 1.44)^2$. As shown in the figure, the two sets of data agree well. The areal magnification function decreased systematically with an increase in eccentricity. Three-way (2 hemispheres, 8 eccentricities, 2 anatomical positions) repeated-measures analysis of variance (ANOVA; p values calculated using Greenhouse–Geisser correction) revealed no significant difference between the left and right hemisphere V1 areal magnification factors [F(1, 21) = 4.248; P = 0.299]. Differences were significant between the dorsal and ventral region V1 areal magnification factors [F(1, 21) = 1.894; $P < 0.05$].

5. DISCUSSION

Our results indicate that the most peripheral representation locates in the fundus of the POS. Previous fMRI studies of human retinotopic mapping have identified the V1 using the visual stimulus limited to the central and/or peri-central visual field[4-6,15,16]. The stimuli used did not directly activate much of the periphery in V1, and it was hard to compare with physiological studies of human peripheral vision above 30° of eccentricity. Using wide-view visual presentation system, we estimated that the V1 has an average surface size of approximately 2229 mm^2, which represents the portion of visual field eccentricity

from 0° to 60°. Our estimates are consistent with the results of other physiological and fMRI studies[9,17-20].

Some studies using retinotopic mapping data from macaques have attempted to mathematically model how areal cortical magnification varies as a function of eccentricity[21-23], giving a general function of $M = a (b + E) c$, where E is eccentricity in degrees, and a, b, and c are constants. Assuming that the visual field map in the V1 conforms to pure logarithmic conformal mapping, the constant c would equal –2 for areal cortical magnification. This function fit the present data very well, using the parameters $a = 272$ and $b = 1.44$ for the V1. Horton and Hoyt proposed that the function $M_{areal} = 300/(E + 0.75)^2$ describes the human areal cortical magnification factor for V1 (Horton and Hoyt, 1991). Our results for area cortical magnification are in close agreement with theirs. If we assume that human linear cortical magnification is isotropic in the V1, the square root of the present areal cortical magnification function yields the following expression for the linear cortical magnification factor: $M_{linear} = 16.5/(E + 1.44)$. Results using this equation agree closely with various previous measurements of visual field representation from 0 degress to 12 degrees[4,24]. In present study, we quantitatively investigated the properties of peripheral visual field representation, which provided basic data to make detailed predictions about the behavior of a human peripheral visual field of V1.

Humans rely on their eyes to obtain visual information and the visual information is in direct proportion to the area of the visual field. The area of cortical magnification is defined as the area of the cortical surface area of the visual field. Therefore, the cortical magnification factor is correlated with the characteristics of the visual field. As shown in Figure 7, the magnification is larger in lower eccentricity (under 12degrees) which was defined as central vision and smaller in higher eccentricity (above 12 degrees) which was defined as peripheral vision. When the eccentricity is above 12 degrees, the magnification is down to 1 mm² per degree². That is, large cortical area needs to process the visual information from the central visual field, but small cortical area processes the visual information from the peripheral visual field which the area is significantly larger than the central. Humans rely on central vision to obtain important visual information and most visual information from the peripheral vision could not be processed efficiently. At the crossroad intersection, drivers need to observe the surrounding situation of both sides by peripheral vision. But in the human visual cortex, only a small cortical area is used to process visual information from the peripheral visual field. There-
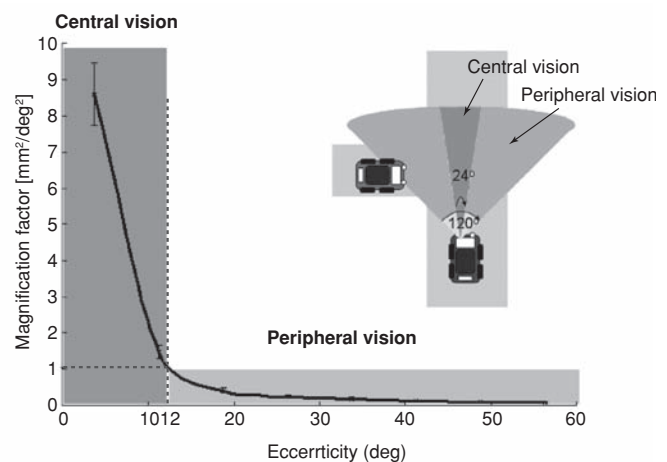

Fig. 7 The correlation of cortical magnification factor and traffic safety. The top-right graph is an example that two cars meet at a crossroad intersection. The light color area is the central vision of the driver of the blue car. The deep color area is the peripheral vision of the driver. When cars meet at the intersection, the driver usually observes the situation by peripheral vision. But there is a low cortical magnification factor in the peripheral vision. That is, only a small cortical area processes the visual information from the peripheral visual field which has large visual information and most visual information from the peripheral vision could not be processed efficiently.

fore, crossroad intersections are more prone to traffic accidents, particularly in the narrow mouth of the road while the driver needs the vision of greater eccentricity on both sides to observe the road situation.

6. CONCLUSION

In this study, we quantitatively investigated the functional characteristics of human peripheral visual fields by fMRI. We analyzed the fMRI data to identify the areal magnification factor and surface area size of the V1 for a wide visual field of eccentricity up to 60° which is larger than that in previous studies. Our experimental results indicate that the function $M_{areal} = 272/(E + 1.44)^2$ describes the human areal cortical magnification factor of the V1 for an eccentricity of 0° to 60°. We also estimated the average V1 surface area to be approximately 2229 mm². This study demonstrated that by using wide-range visual stimuli, fMRI studies can obtain results and provide basic data to make detailed predictions about the behavior of a human peripheral visual field of V1.

From the results of this study, we can explain why traffic accidents easily take place at road intersections. This is because the cortical area, which is used to process visual information from peripheral visual field, is very small, hence drivers cannot notice the danger from both sides by peripheral vision. It is suggested that more obvious warning signs should be installed in the central visual field for drivers. In a narrow junction, drivers must be trained to move their eyes rapidly and glance around to view the situation on both sides.

REFERENCES

1. White paper on traffic safety in Japan, Part 1, Chapter 1. (2008).
2. Burton KB, Owsley C, Sloane ME. Aging and neural spatial contrast sensitivity: photopic vision. "Vision Research" 33: pp.939–946. (1993).
3. Gao H, Hollyfield J G. Aging of the human retina: differential loss of neurones and retinal epithelial cells. "Investigative Ophthalmology and Visual Science" 33: pp.1–17. (1992).
4. Engel SA, Glover GH, Wandell BA. Retinotopic organization in human visual cortex and the spatial precision of functional MRI. "Cereb Cortex" 7: pp.181-192. (1997).
5. Sereno MI, Dale AM, Reppas JB, Kwong KK, Belliveau JW, Brady TJ, et al. Borders of multiple visual areas in humans revealed by functional magnetic resonance imaging. "Science" 268: pp.889-893. (1995).
6. DeYoe EA, Carman GJ, Bandettini P, Glickman S, Wieser J, Cox R, et al. Mapping striate and extrastriate visual areas in human cerebral cortex. "Proc Natl Acad Sci USA" 93: pp.2382-2386. (1996).
7. Daniel PM, Whitteridge D. The representation of the visual field on the cerebral cortex in monkeys. "J Physiol" 159: pp.203-221. (1961).
8. Duncan RO, Boynton GM. Cortical magnification within human primary visual cortex correlates with acuity thresholds. "Neuron" 38: pp.659-671. (2003).
9. Smith AT, Singh KD, Williams AL, Greenlee MW. Estimating receptive field size from fMRI data in human striate and extrastriate visual cortex. "Cereb Cortex" 11: pp.1182-1190. (2001).
10. Goebel R, Khorram-Sefat D, Muckli L, Hacker H, Singer W. The constructive nature of vision: direct evidence from functional magnetic resonance imaging studies of apparent motion and motion imagery. "Eur J Neurosci" 10: pp.1563-1573. (1998).
11. Lu H, Basso G, Serences JT, Yantis S, Golay X, van Zijl PC. Retinotopic mapping in the human visual cortex using vascular space occupancy-dependent functional magnetic resonance imaging. "Neuroreport" 16: pp.1635-1640. (2005).
12. Fischl B, Dale AM. Measuring the thickness of the human cerebral cortex from magnetic resonance images. "Proc Natl Acad Sci USA" 97: pp.11050-11055. (2000).
13. Myerson J, Manis PB, Miezin FM, Allman JM. Magnification in striate cortex and retinal ganglion cell layer of owl monkey: a quantitative comparison. "Science" 198: pp.855-857. (1977).
14. Horton JC, Hoyt WF. The representation of the visual field in human striate cortex. A revision of the classic Holmes map. "Arch Ophthalmol" 109: pp.816-824. (1991).
15. Pitzalis S, Galletti C, Huang RS, Patria F, Committeri G, Galati G, et al. Wide-field retinotopy defines human cortical visual area v6. "J Neurosci" 26: pp.7962-7973. (2006).
16. Stenbacka L, Vanni S. Central luminance flicker can activate peripheral retinotopic representation. "Neuroimage" 34: pp.342-348. (2007).
17. Andrews TJ, Halpern SD, Purves D. Correlated size variations in human visual cortex, lateral geniculate nucleus, and optic tract. "J Neurosci" 17: pp.2859-2868. (1977).
18. Stensaas SS, Eddington DK, Dobelle WH. The topography and variability of the primary visual cortex in man. "J Neurosurg" 40: pp.747-755. (1974).
19. Adams DL, Horton JC. A precise retinotopic map of primate striate cortex generated from the representation of angioscotomas. "J Neurosci" 23: pp.3771-3789. (2003).
20. Dougherty RF, Koch VM, Brewer AA, Fischer B, Modersitzki J, Wandell BA. Visual field representations and locations of visual areas V1/2/3 in human visual cortex. "J Vis" 3: pp.586-598. (2003).
21. Van Essen DC, Newsome WT, Maunsell JH. The visual field representation in striate cortex of the macaque monkey: asymmetries, anisotropies, and individual variability. "Vision Res"24: pp.429-448. (1984).
22. LeVay S, Connolly M, Houde J, Van Essen DC. The complete pattern of ocular dominance stripes in the striate cortex and visual field of the macaque monkey. "J Neurosci" 5: pp.486-501. (1985).
23. Ejima Y, Takahashi S, Yamamoto H, Fukunaga M, Tanaka C, Ebisu T, et al. Interindividual and interspecies variations of the extrastriate visual cortex. "Neuroreport" 14: pp.1579-1583. (2003).
24. Qiu A, Rosenau BJ, Greenberg AS, Hurdal MK, Barta P, Yantis S, et al. Estimating linear cortical magnification in human primary visual cortex via dynamic programming. "Neuroimage" 31: pp.125-138. (2006).

ACKNOWLEDGEMENTS